ARTICLE

First Principles Study of Uranium Solubility in $Gd_2Zr_2O_7$ Pyrochlore

Qing-yun Chen[a], Kai-min Shih[b*], Chuan-min Meng[c*], Lie-lin Wang[a], Hua Xie[a], Tao Wu[a]

a. Key Subject Laboratory of National Defense for Radioactive Waste and Environmental Security, Southwest University of Science and Technology, Mianyang 621010, China
b. Department of Civil Engineering, The University of Hong Kong, Pokfulam Road, Hong Kong SAR, China
c. Key Lab for Shock Wave and Detonation Physics Research, Institute of Fluid Physics, Chinese Academy of Engineering Physics, Mianyang 621900

(Dated: Received on June 8, 2015; Accepted on August 1, 2015)

Ab initio calculation is performed to investigate the uranium solubility in different sites of $Gd_2Zr_2O_7$ pyrochlore. The $Gd_2Zr_2O_7$ maintains its pyrochlore structure at low uranium dopant levels, and the lattice constants of $Gd_2(Zr_{2-y}U_y)O_7$ and $(Gd_{2-y}U_y)Zr_2O_7$ are generally expressed as being linearly related to the uranium content y. Uranium is found to be a preferable substitute for the B-site gadolinium atoms in cation-disordered $Gd_2Zr_2O_7$ (where gadolinium and zirconium atoms are swapped) over the A-site gadolinium atoms in ordered $Gd_2Zr_2O_7$ due to the lower total energy of $(Gd_{2-y}Zr_y)(Zr_{2-y}U_y)O_7$.

Key words: $Gd_2Zr_2O_7$ pyrochlore, Nuclear waste, Uranium solubility, Density functional theory

I. INTRODUCTION

The emergence of nuclear energy offers promising opportunities for the development of inexpensive and highly efficient energy sources. However, the safe disposal of large amounts of nuclear waste, especially long-lived radioactive elements, remains an important challenge for the nuclear industry [1, 2]. Gadolinium zirconate ($Gd_2Zr_2O_7$) pyrochlore exhibits high chemical durability, radiation resistance, and solubility for large radionuclide species (such as thorium, uranium, and plutonium) and is therefore an attractive candidate as a nuclear-waste host material [3−9].

In an ordered $A_2B_2O_7$ pyrochlore structure (space group Fd3m) with A (gadolinium or rare earths) and B (zirconium, titanium, tin, hafnium, or plumbum) cations ordered on the 16d (0.5, 0.5, 0.5) and 16c (0, 0, 0) sites, respectively, oxygen can be found at the 48f (x, 0.125, 0.125) and 8b (0.375, 0.375, 0.375) positions. The 8a (0.125, 0.125, 0.125) site is vacant (using the Wyckoff notation) [10, 11]. $Gd_2Zr_2O_7$ crystallizes in the cubic pyrochlore structure, and large quantities of act inide elements are expected to be incorporated into the matrix at both the gadolinium and zirconium lattice positions [12−15].

Sickafus *et al.* [6] concluded that the use of radiation-tolerant materials in the 2:2:7 pyrochlore stoichiometry phase presented no advantage. The key to radiation tolerance is an inherent ability to accommodate atomic lattice disorder. Under ion irradiation, the ordered pyrochlore superstructure is transformed into an anion-disordered pyrochlore before its final transformation into a cation-disordered defect-fluorite structure type [16]. It has been shown that $Gd_2Zr_2O_7$ is transformed into a radiation-resistant anion-deficient fluorite structure upon irradiation and shows greater radiation resistance than $Gd_2Ti_2O_7$, which has greater defect formation energy disorder and is more susceptible to amorphization [3]. Regarding the primacy of cation or anion disorders, inconsistent conclusions can be obtained. For example, diffraction studies indicated that oxygen disorder caused cation disorder, while spectroscopy studies yielded the opposite conclusion [11]. Although the underlying mechanisms of defect formation and radiation resistance are not yet well understood, there is a consensus that the accommodation of lattice disorder should improve amorphization resistance in a displacive radiation damage environment [3, 6, 10].

Kulkarni *et al.* [17] reported that plutonium can completely replace gadolinium (A site) in a $Gd_2Zr_2O_7$ matrix. However, uranium can replace only 40% of the gadolinium at the A site in the $Gd_2Zr_2O_7$ matrix, while it can replace all of the zirconium at the B site. The structure of $Gd_2Zr_2O_7$ is transformed from a pyrochlore into a closely related fluorite structure as the level of uranium dopant increases [12]. By controlling the sintering atmosphere, uranium with various oxidation states and ionic radii can be incorporated into a $Gd_2Zr_2O_7$ matrix along with pyrochlore and defect fluorite structures [18].

Gregg *et al.* [19] recently examined U-doped and off-

*Authors to whom correspondence should be addressed. E-mail: kshih@hku.hk, mcm901570@126.com

stoichiometric $Gd_2Zr_2O_7$ pyrochlore via X-ray diffraction (XRD) and X-ray absorption near-edge structure (XANES) spectroscopy. They suggested that uranium cations are largely located at pyrochlore B sites instead of the targeted A sites. The study provided direct evidence for cation antisite disorder in U-doped $Gd_2Zr_2O_7$ pyrochlore [19]. Although some experimental studies have considered a solution of high-level radioactive-waste uranium in $Gd_2Zr_2O_7$ pyrochlores, the mechanisms that underlie uranium doping and disorder (defect formation) in $Gd_2Zr_2O_7$ crystals are not yet well understood.

First principles density functional theory (DFT) simulations have become ideal tools for the systematic investigation of properties other than chemical compositions. In this work, the virtual crystal approximation (VCA) method is used to calculate the total energies and structure properties of U-doped $Gd_2Zr_2O_7$ pyrochlores (ordered and cation-disordered structures). The solution behavior of uranium in $Gd_2Zr_2O_7$ pyrochlores is also clarified.

II. COMPUTATIONAL METHOD

The calculations are performed using the first-principles plane-wave pseudopotential method based on DFT incorporated into the CASTEP computational code [20]. The exchange-correlation energy of the electrons is described according to the local-density approximation (LDA) framework [21]. The Coulomb potential energy caused by electron-ion interaction is described with the ultrasoft scheme, in which the orbits of Gd($4f^7$, $5s^2$, $5p^6$, $5d^1$, $6s^2$), Zr($4s^2$, $4p^6$, $4d^2$, $5s^2$), U($5f^3$, $6s^2$, $6p^6$, $6d^1$, $7s^2$), and O($2s^2$, $2p^4$) are treated as valence electrons. The electronic wave functions are expanded in a plane wave basis set with an energy cutoff of 500 eV. A Monkhorst-Pack mesh with 3×3×3 k-points is used for Brillouin-zone k-point sampling, and the self-consistent convergence of total energy is 2×10^{-6} eV/atom. These parameters are sufficient to achieve well-converged total energy and geometric configurations.

The VCA method is used to model four series of configurations, including $(Gd_{2-y}U_y)Zr_2O_7$, $Gd_2(Zr_{2-y}U_y)O_7$, $(Gd_{2-y}Zr_y)(Zr_{2-y}Gd_y)O_7$, and $(Gd_{2-y}Zr_y)(Zr_{2-y}U_y)O_7$, to study the solution behavior of uranium at various sites on a $Gd_2Zr_2O_7$ lattice. The VCA in CASTEP is capable of correct describing a number of mixture atoms [22]. The VCA method performed well even when applied to elements that were far apart on the periodic table [23−26]. The atomic sites in a disordered crystal can be described in terms of a hybrid atom that consists of two element types. The relative concentrations can be set for any number of atoms, and the total concentration must be 100%. Using the VCA method, the uranium atoms can be distributed randomly in the $Gd_2Zr_2O_7$ lattice, and any percentage of uranium content can be introduced to the disordered system.

The full structural relaxations for all of the configurations are performed first. During structure optimization, the total energy is minimized by varying the lattice constants according to the restrictions of the given symmetry. The crystal and electronic structures of all series are then calculated. Because structural phase changes from pyrochlore to fluorite are observed at higher y values [12], y=0 to 0.4 for all series in this study. The VCA method is adopted, according to which the uranium atoms that occupy the lattice site are described via the index y (*i.e.*, the atomic fraction of uranium at the lattice site) to model the solubility of the uranium in the $Gd_2Zr_2O_7$ pyrochlore. The calculation results are given as statistical average values.

III. RESULTS AND DISCUSSION

Table I presents the lattice constants, internal positional parameter x_{O48f}, and bond distances between the nearest-neighboring cations and anions of the $Gd_2Zr_2O_7$ pyrochlore. The calculated lattice constants a and x_{O48f} are 10.37 Å and 0.340, respectively, and are therefore in agreement with the experimental [4, 18] and other calculated [10, 28, 29] results. The bond distances between the nearest-neighboring cations and anions are also in agreement with other results [4]. The tight-binding (TB) [10] and DFT with energy correction (DFT+U) approaches [28] exhibit greater lattice constants and bond lengths of $Gd_2Zr_2O_7$ pyrochlore. Although the TB approach is based on quantum mechanics, it lacks reliability and transferability due to the parameterization of the electronic Hamiltonian with a finite set of equilibrium structures and properties, and even lacks self-consistency in most cases.

The cubic lattice constant and positional parameter of x_{O48f} can be used to completely describe the pyrochlore structure. Figure 1(a) exhibits the calculated lattice constants a as a function of the uranium content y in $(Gd_{2-y}U_y)Zr_2O_7$ and $Gd_2(Zr_{2-y}U_y)O_7$ to clarify the fundamental properties of U-doped gadolinium zirconate pyrochlore. Vegard's law is valid below y=0.3, and the lattice constants of $Gd_2(Zr_{2-y}U_y)O_7$ and $(Gd_{2-y}U_y)Zr_2O_7$ are generally expressed as possessing a linear relationship to the uranium content y. Although the lattice constants of $Gd_2(Zr_{2-y}U_y)O_7$ increase with the enriched uranium content, the $(Gd_{2-y}U_y)Zr_2O_7$ series shows the opposite tendency.

It has been observed that the increase in the lattice constant of $(Gd_{2-y}U_y)Zr_2O_7$ is related to the difference in the ionic radii of the gadolinium and uranium ions and that the decrease of $Gd_2(Zr_{2-y}U_y)O_7$ is related to the incorporation of the larger uranium ion at the zirconium site [12]. The differences between the calculated lattice parameter and the available experimen-

DOI:10.1063/1674-0068/28/cjcp1506121

TABLE I The lattice constants, internal positional parameters x_{O48f}, and bond distances between the nearest-neighboring cations and anions of the $Gd_2Zr_2O_7$ pyrochlore.

	a/Å	x_{O48f}	d_{Gd-O8b}/Å	$d_{Gd-O48f}$/Å	$d_{Zr-O48f}$/Å
LDA	10.37	0.340	2.246	2.470	2.060
Expt.	10.54 [4]	0.344 [4]		2.483 [4]	2.110 [4]
	10.53 [18]				
Other calc.	10.535 [10]	0.374 [10]	2.281 [10]	2.462 [10]	2.125 [10]
	10.66 [28]	0.339 [28]	2.307 [28]	2.548 [28]	2.110 [28]
	10.76 [29]				

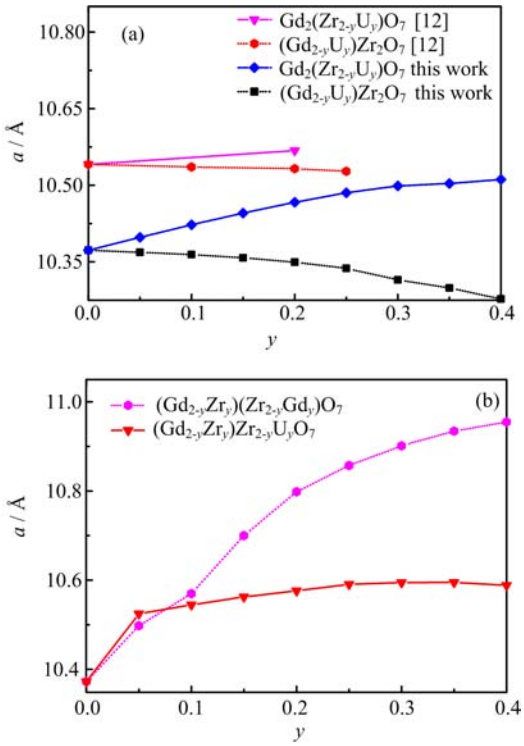

FIG. 1 The calculated lattice constants a as a function of y in $(Gd_{2-y}U_y)Zr_2O_7$, $Gd_2(Zr_{2-y}U_y)O_7$, and $(Gd_{2-y}Zr_y)(Zr_{2-y}U_y)O_7$ and cation disorder parameter y in $(Gd_{2-y}Zr_y)(Zr_{2-y}Gd_y)O_7$. (a) Lattice constants a of $(Gd_{2-y}U_y)Zr_2O_7$ and $Gd_2(Zr_{2-y}U_y)O_7$ compared with those results in Ref.[12], and (b) lattice constants a of $(Gd_{2-y}Zr_y)(Zr_{2-y}U_y)O_7$ and $(Gd_{2-y}Zr_y)(Zr_{2-y}Gd_y)O_7$.

tal results are all within 1.7%, which indicates that the calculation results of the current study are fairly trustworthy. The lattice expansion is obviously expressed along with the degree of cation disorder, as shown in Fig.1(b). Previous studies have also expressed linear lattice constants related to the indium composition x in $In_xAl_{1-x}N$ and to the cation disorder index x in $(Mg_{1-x}Al_x)[Mg_xAl_{2-x}]O_4$ [30, 31].

The lattice constants present obvious variations when y>0.4 (data not shown). The variation mainly involves the loss of pyrochlore ordering above this concentration level [12]. Therefore, the pyrochlore structure model for high uranium content is not suitable. The results of y<0.2 are considered in the following discussion.

Figure 2 shows the variations in the optimized bond length as a function of the uranium content y or cation disorder parameter y. Although the bond length between O and its nearest-neighboring cations gradually increases with increasing uranium content in $Gd_2(Zr_{2-y}U_y)O_7$, the opposite holds true for $(Gd_{2-y}U_y)Zr_2O_7$. No obvious changes in the bond length between the O- and B-site cations are observed. The bond lengths d_{A-O8b} and d_{B-48f} obviously increase along with the increasing cation disorder parameter y in $(Gd_{2-y}Zr_y)(Zr_{2-y}U_y)O_7$. The change in the tendency of the lattice parameters (see Fig.1) is similar to the change in the tendency of d_{A-O8b} (the bond length between the A-site cation and O8b) and d_{B-O48f} (the bond length between the B-site cation and O_{48f}), exhibiting a certain regularity and a preferable relativity. The lattice constant of the pyrochlore is determined by d_{A-O48f} and d_{B-O48f}, which are short bond lengths that exhibit strong interactions between the related atoms.

The electron density difference is typically the difference between an assumed standard or model electron density and the actual observed or DFT-computed electron density. The difference provides information related to electron transfer and distribution after bonding. The electron density differences of $Gd_2Zr_2O_7$, $Gd_2(Zr_{2-y}U_y)O_7$, $(Gd_{2-y}U_y)Zr_2O_7$, $(Gd_{2-y}Zr_y)(Zr_{2-y}Gd_y)O_7$, and $(Gd_{2-y}Zr_y)(Zr_{2-y}U_y)O_7$ are shown in Fig.3, in which the bright (red) and darker (blue) areas indicate positive and negative electron transfer, respectively.

In general, a covalent interaction exists between the B-site cations and the nearest-neighboring O, and an ionic interaction exists between the A-site cations and the nearest-neighboring O. No obvious electronegativity changes are seen in $(Gd_{2-y}U_y)Zr_2O_7$ and $Gd_2(Zr_{2-y}U_y)O_7$. The changes in the lattice constants of $(Gd_{2-y}U_y)Zr_2O_7$ and $Gd_2(Zr_{2-y}U_y)O_7$ are related to the difference in the change in the ionic radii after doping. Furthermore, the lattice-constant changes of $(Gd_{2-y}Zr_y)(Zr_{2-y}Gd_y)O_7$ and $(Gd_{2-y}Zr_y)(Zr_{2-y}U_y)O_7$ are related to the electronegativity change of the cation sites that arise from atom swapping or doping.

DOI:10.1063/1674-0068/28/cjcp1506121

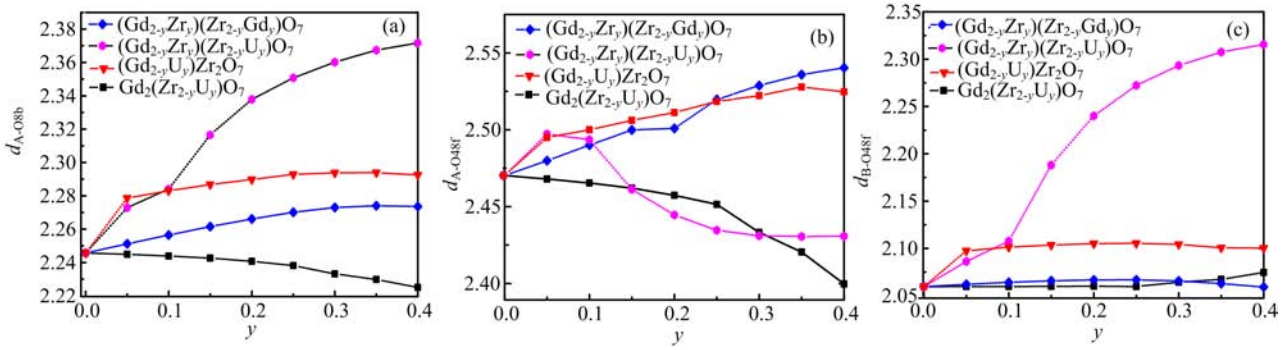

FIG. 2 The variations in the optimized bond length as a function of y in $(Gd_{2-y}U_y)Zr_2O_7$, $Gd_2(Zr_{2-y}U_y)O_7$ and $(Gd_{2-y}Zr_y)(Zr_{2-y}U_y)O_7$ and cation disorder parameter y in $(Gd_{2-y}Zr_y)(Zr_{2-y}Gd_y)O_7$. (a) d_{A-O8b}, (b) d_{A-48f}, and (c) d_{B-48f}.

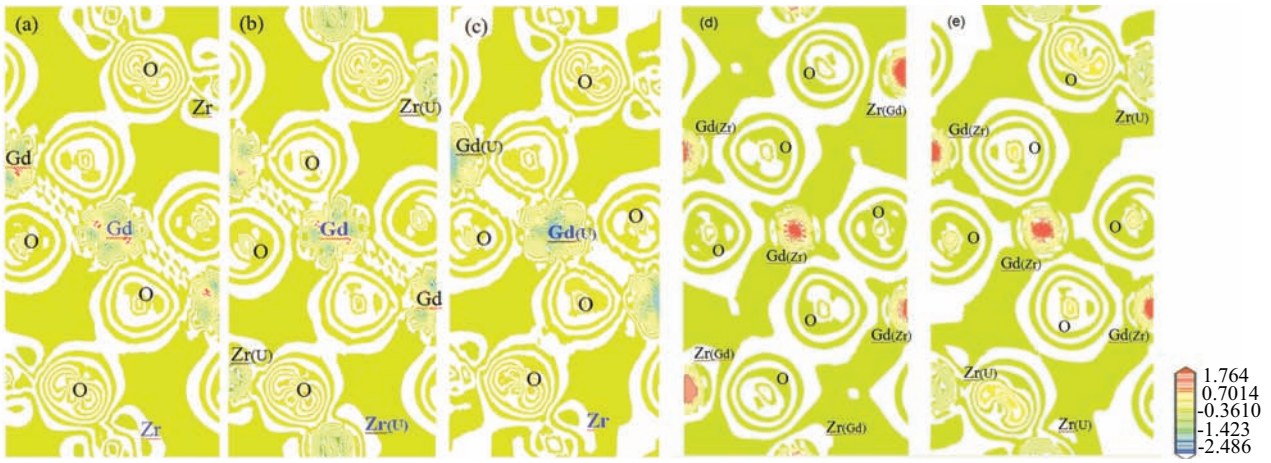

FIG. 3 Electron density difference of (a) $Gd_2Zr_2O_7$, (b) $Gd_2(Zr_{2-y}U_y)O_7$, (c) $(Gd_{2-y}U_y)Zr_2O_7$, (d) $(Gd_{2-y}Zr_y)(Zr_{2-y}Gd_y)O_7$, and (e) $(Gd_{2-y}Zr_y)(Zr_{2-y}U_y)O_7$.

A high level of Coulomb repulsion exists between two atoms with high electronegativity. As shown in Fig.3(d), the A-site electronegativity in the $(Gd_{2-y}Zr_y)(Zr_{2-y}Gd_y)O$ lattice obviously increases (*i.e.*, more red areas) due to cation disorder. The Coulomb repulsion between the A-site atoms and O_{8b} increases, and the ionic bond d_{A-O8b} increases while the Coulomb repulsions are dominant. The covalent bond plays a dominant role in the bond d_{B-O48f}, which increases due to the introduction of atoms with larger ionic radii in the B sites.

The lattice constant of pyrochlore is determined by the short bond lengths d_{A-O8b} and d_{B-O48f}. Therefore, the lattice parameter of $(Gd_{2-y}Zr_y)(Zr_{2-y}Gd_y)O_7$ obviously increases with the increase in cation disorder, and the $(Gd_{2-y}Zr_y)(Zr_{2-y}U_y)O_7$ case has fewer lattice parameter increases due to the less increase in electronegativity in the B-site atoms.

The total energy of $(Gd_{2-y}U_y)Zr_2O_7$ and $(Gd_{2-y}Zr_y)(Zr_{2-y}U_y)O_7$ gradually increases with the uranium content y (see Fig.4). With the increase of cation disorder y, the total energy of $(Gd_{2-y}Zr_y)(Zr_{2-y}Gd_y)O_7$ increases linearly, which suggests the instability of the higher cation disorder. This finding is comparable with the total energy difference between $(Gd_{2-y}U_y)Zr_2O_7$ and $(Gd_{2-y}Zr_y)(Zr_{2-y}U_y)O_7$ of the same uranium content y, as the two structures have the same numbers and kinds of atoms. $(Gd_{2-y}Zr_y)(Zr_{2-y}U_y)O_7$ structures have lower total energy and are more stable than $(Gd_{2-y}U_y)Zr_2O_7$ structures when the y values are the same.

Studies using synchrotron XRD, XANES, and positron annihilation lifetime spectroscopy have suggested that the uranium cation in doped gadolinium zirconates ($Gd_{2-x}U_xZr_2O_7$, x=0.1 and 0.2) is largely located at the pyrochlore B site instead of at the targeted A site [19]. Based on the total energy calculation, uranium is a more preferable substitute for the B-site gadolinium atoms in cation-disordered $Gd_2Zr_2O_7$ than for the A-site gadolinium atoms in ordered $Gd_2Zr_2O_7$ due to the former's lower total energy. Finally, there is little total energy variation in $(Gd_{2-y}Zr_y)(Zr_{2-y}U_y)O_7$ due to the small differences in the atomic energy and

DOI:10.1063/1674-0068/28/cjcp1506121

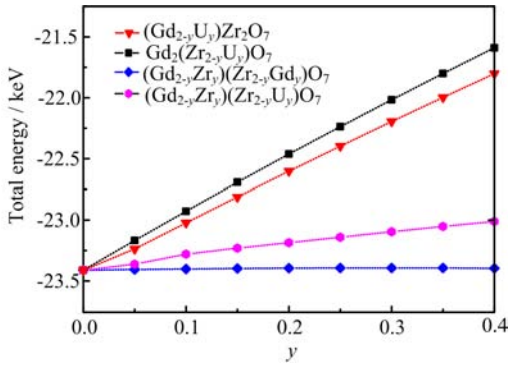

FIG. 4 Total energy as a function of y (uranium content and cation disorder parameter).

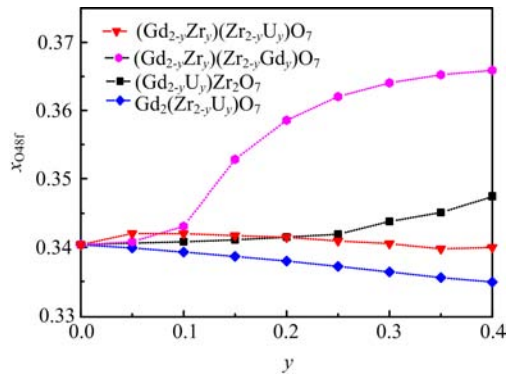

FIG. 5 The O_{48f} positional parameter x (x_{O48f}) as a function of y (uranium content and cation disorder parameter).

ionic radius between zirconium and uranium [32].

All of the atoms in an ideal pyrochlore, with the exception of 48f (O_{48f}), are located at special positions. Thus, the structure is completely described by the lattice parameter a and the fractional coordinate x of O_{48f} [33]. The O_{48f} positional parameter x (x_{O48f}) is an important indicator of a pyrochlore's degree of disorder and resistance to irradiation-induced amorphization [34]. As shown in Fig.5, the x_{O48f} values of a U-doped pyrochlore do not obviously change with an increase in the uranium content. This finding suggests that the gadolinium zirconate pyrochlore is a good uranium immobilization matrix that can maintain its radiation tolerance in the case of low uranium content doping. The x_{O48f} values of the cation disorder series $(Gd_{2-y}Zr_y)(Zr_{2-y}U_y)O_7$ obviously increase when y>0.1.

Lian *et al.* observed that the radiation resistance of pyrochlore was closely related to the cation ionic radius ratio and x positional parameter x_{O48f} [35]. A decrease in the average ionic radius ratio of the A and B sites (r_A/r_B) generally leads to a decrease in the critical temperature for amorphization and a resistance to radiation damage. Furthermore, the radiation resistance of $Gd_2(Ti_{1-x}Zr_x)_2O_7$ increases as the concentration of zirconium increases [36]. The high radiation resistance of $Gd_2Zr_2O_7$ is caused not only by the high neutron absorption cross-section of gadolinium, but also by the transformation of the pyrochlore structure into a defect-fluorite structure, with the disordering of cation antisite defects (A and B cations that exchange places) coupled with the disordering of oxygen Frenkel pairs (a 48f oxygen is moved to an adjacent empty 8a site, resulting in a vacant 48f oxygen site and an occupied 8a oxygen site).

Gregg *et al.* [19] suggested that cation disordering is important to increase ionic conductivity and increase resistance to radiation-induced amorphization in pyrochlores. Pyrochlores have the general formula $A_2B_2O_7$, in which A is usually occupied by the larger cation and B is occupied by the smaller cation. The stability of the pyrochlore structure is governed by the ionic radii ratio of the A to B cations (r_A/r_B) [10], which is affected by the disorder, the ionic value, and the substitution site of the doping atom. The high radiation resistance of the $Gd_2Zr_2O_7$ pyrochlore can be attributed to the similar ion radii of the A- and B-site atoms, which easily change into highly radiation-resistant fluorite structures [3]. It has been consistently concluded that the radii ratio of the A to B sites (r_A/r_B) decreases as y increases in $(Gd_{2-y}Zr_y)(Zr_{2-y}Gd_y)O_7$. Furthermore, the positional parameter x_{O48f} increases and shows greater radiation resistance capability.

IV. CONCLUSION

In this work, the VCA method is used to calculate the total energy and structural properties of U-doped $Gd_2Zr_2O_7$ pyrochlores (*i.e.*, both ordered and cation-disordered structures). The $Gd_2Zr_2O_7$ maintains its pyrochlore structure at low uranium dopant levels, and the lattice constants of $Gd_2(Zr_{2-y}U_y)O_7$ and $(Gd_{2-y}U_y)Zr_2O_7$ are generally expressed as a linear Vegard's relationship to the uranium content y. As the uranium content is enriched, the lattice constants of $Gd_2(Zr_{2-y}U_y)O_7$ increase. However, the $(Gd_{2-y}U_y)Zr_2O_7$ series exhibits the opposite tendency. These results are in agreement with those of previous experiments.

The lattice-constant changes of $(Gd_{2-y}U_y)Zr_2O_7$ and $Gd_2(Zr_{2-y}U_y)O_7$ are related to the difference in the ionic radii change after doping. The lattice-constant changes of $(Gd_{2-y}Zr_y)(Zr_{2-y}Gd_y)O_7$ and $(Gd_{2-y}Zr_y)(Zr_{2-y}U_y)O_7$ are related to the change in electronegativity of the cation sites that arise from the swapping or doping of atoms. In the case of $(Gd_{2-y}Zr_y)(Zr_{2-y}Gd_y)O_7$, the Coulomb repulsions between the A-site atoms and the O_{8b}-site increase, and the ionic bond d_{A-O8b} increases while the Coulomb repulsions are dominant. The covalent bond plays a dominant role in the bond d_{B-O48f}, which increases due to the introduction of atoms with larger ionic radii. The lattice constant of pyrochlore is determined by the short

DOI:10.1063/1674-0068/28/cjcp1506121

bond lengths of $d_{\mathrm{A-O8b}}$ and $d_{\mathrm{B-O48f}}$. Therefore, the lattice parameter obviously increases along with an increase in cation disorder in $(Gd_{2-y}Zr_y)(Zr_{2-y}Gd_y)O_7$, and a smaller lattice parameter increase is seen in $(Gd_{2-y}Zr_y)(Zr_{2-y}U_y)O_7$ due to the lower increase in electronegativity at the B site. The radii ratio of the A to B sites (r_A/r_B) decreases as the cation disorder y in $(Gd_{2-y}Zr_y)(Zr_{2-y}Gd_y)O_7$ increases. Furthermore, the positional parameter x_{O48f} increases, which indicates greater radiation resistance capability. Finally, uranium is a preferable substitute for the B-site gadolinium atoms in cation-disordered $Gd_2Zr_2O_7$ over the A-site gadolinium atoms in ordered $Gd_2Zr_2O_7$ due to the former's lower total energy.

V. ACKNOWLEDGMENTS

This work was supported by the General Research Fund Scheme of the Research Grants Council of Hong Kong (No.715612 and No.17206714), the National Natural Science Foundation of China (No.11304254 and No.21101129), and the Key Subject Laboratory Foundation of National Defense for Radioactive Waste Environmental Security of SWUST (No.13zxnk09 and No.13zxnk11).

[1] J. Tollefson, Nature **473**, 266 (2011).
[2] R. C. Ewing, Proc. Natl. Acad. Sci. USA **96**, 3432 (1999).
[3] K. E. Sickafus, L. Minervini, R. W. Grimes, J. A. Valdez, M. Ishimaru, F. Li, K. J. McClellan, and T. Hartmann, Science **289**, 748 (2000).
[4] B. P. Mandal and A. K. Tyagi, J. Alloys Comp. **437**, 260 (2007).
[5] J. Lian, L. M. Wang, S. X. Wang, J. Chen, L. A. Boatner, and R. C. Ewing, Phys. Rev. Lett. **87**, 145901 (2001).
[6] K. E. Sickafus, R. W. Grimes, J. A. Valdez, A. Cleave, M. Tang, M. Ishimaru, S. M. Corish, C. R. Stanek, and B. P. Uberuaga, Nat. Mater. **6**, 217 (2007).
[7] S. Moll, G. Sattonnay, L. Thomé, J. Jagielski, C. Decorse, P. Simon, I. Monnet, and W. J. Weber, Phys. Rev. B **84**, 064115 (2011).
[8] S. J. Patwe, B. R. Ambekar, and A. K. Tyagi, J. Alloys Comp. **389**, 243 (2005).
[9] R. C. Ewing, W. J. Weber, and J. Lian, J. Appl. Phys. **95**, 5949 (2004).
[10] G. Sattonnay and R. Tétot, J. Phys.: Condens. Matter **26**, 055403 (2014).
[11] W. R. Panero, L. Stixrude, and R. C. Ewing, Phys. Rev. B **70**, 054110 (2004).
[12] K. V. G. Kutty, R. Asuvathraman, R. R. Madhavan, and H. Jena, J. Phys. Chem. Solids **66**, 596 (2005).
[13] J. D. S. Walker, J. R. Hayes, M. W. Gaultois, E. R. Aluri, and A. P. Grosvenor, J. Alloys Comp. **565**, 44 (2013).
[14] A. Garbout, B. Bouattour, and A. W. Kolsi, J. Alloys Comp. **469**, 229 (2009).
[15] Z. Liu, S. Gao, J. Ouyang, and X. Xia, J. Alloys Comp. **506**, 868 (2010).
[16] J. Lian, L. Wang, J. Chen, K. Sun, R. C. Ewing, J. Matt Farmer, and L. A. Boatner, Acta Mater. **51**, 1493 (2003).
[17] N. K. Kulkarni, S. Sampath, and V. Venugopal, J. Nucl. Mater. **281**, 248 (2000).
[18] D. J. Gregg, Y. Zhang, Z. Zhang, I. Karatchevtseva, M. G. Blackford, G. Triani, G. R. Lumpkin, and E. R. Vance, J. Nucl. Mater. **438**, 144 (2013).
[19] D. J. Gregg, Z. Zhang, G. J. Thorogood, B. J. Kennedy, J. A. Kimpton, G. Griffiths, P. R. Guagliardo, G. R. Lumpkin, and E. R. Vance, J. Nucl. Mater. **452**, 474 (2014).
[20] M. Parrinello and A. Rahman, Phys. Rev. Lett. **45**, 1196 (1980).
[21] S. H. Vosko, L. Wilk, and M. Nusair, Can. J. Phys. **58**, 1200 (1980).
[22] L. Bellaiche and D. Vanderbilt, Phys. Rev. B **61**, 7877 (2000).
[23] A. Gueddima, R. Zerdoumb, and N. Bouarissa, Physica B **389**, 335 (2007).
[24] S. Bacha, A. Bechiri, F. Benmakhlouf, H. Allouache, and N. Bouarissa, Physica B **406**, 2021 (2011).
[25] P. Ou, J. Wang, S. Shang, L. Chen, Y. Du, Z. Liu, and F. Zheng, Surf. Coat. Technol. **264**, 41 (2015).
[26] B. Ghebouli, M. A. Ghebouli, and M. Fatmi, Physica B **406**, 2521 (2011).
[27] B. P. Mandal, A. Banerji, V. Sathe, S. K. Deb, and A. K. Tyagi, J. Solid State Chem. **180**, 2643 (2007).
[28] X. J. Wang, H. Y. Xiao, X. T. Zhu, and W. J. Weber, J. Nucl. Mater. **419**, 105 (2011).
[29] J. A. Purton and N. L. Allan, J. Mater. Chem. **12**, 2923 (2002).
[30] Q. Y. Chen, M. Xu, H. P. Zhou, M. Y. Duan, W. J. Zhu, and H. L. He, Physica B **430**, 1666 (2008).
[31] Q. Y. Chen, C. M. Meng, T. C. Lu, M. Xu, J. Q. Qi, and J. J. Tan, J. Appl. Phys. **108**, 113522 (2010).
[32] R. D. Shannon, Acta Crystallogr. A **32**, 751 (1976).
[33] W. R. Panero, L. Stixrude, and R. C. Ewing, Phys. Rev. B **70**, 054110 (2004).
[34] J. Lian, L. Wang, R. Haire, K. Helean, and R. C. Ewing, Nucl. Instrum. Methods Phys. Res. B **218**, 236 (2004).
[35] J. Lian, S. V. Yudintsev, S. V. stefanovsky, L. M. Wang, R. C. Ewing, J. Alloys Comp. **444-445**, 429 (2007).
[36] S. X. Wang, B. D. Begg, L. M. Wang, R. C. Ewing, W. J. Weber, and K. V. Govidan Kutty, J. Mater. Res. **14**, 4470 (1999).

DOI:10.1063/1674-0068/28/cjcp1506121